

# Nocturnal turbulence at Jezero driven by the onset of a low-level jet as determined from MRAMS modeling and MEDA measurements

J. Pla-García<sup>1</sup>, A. Munguira<sup>2</sup>, S. Rafkin<sup>3</sup>, R. Hueso<sup>2</sup>, A. Sánchez-Lavega<sup>2</sup>, M. de la Torre<sup>4</sup>, D. Viúdez-Moreiras<sup>1</sup>, C. Newman<sup>5</sup>, T. Bertrand<sup>6</sup>, Teresa del Río<sup>2</sup>, N. Murdoch<sup>7</sup>, G. Martínez<sup>8</sup>, H. Savijarvi<sup>9</sup>, B. Chide<sup>7</sup>, M. Richardson<sup>5</sup>, J.A. Rodríguez-Manfredi<sup>1</sup>

<sup>1</sup>Centro de Astrobiología (CSIC- INTA), Madrid, Spain (jpla@cab.inta-csic.es),

<sup>2</sup>Universidad del País Vasco (UPV/EHU), Bilbao, Spain,

<sup>3</sup>Southwest Research Institute, Boulder, CO, USA,

<sup>4</sup>Jet Propulsion Laboratory/California Institute of Technology, Pasadena, CA, USA.

<sup>5</sup>Aeolis Research, Chandler, AZ, USA,

<sup>6</sup>Paris Observatory, France

<sup>7</sup>ISAE-SUPAERO, Université de Toulouse, 31055 Toulouse, France

<sup>8</sup>Lunar and Planetary Institute, Houston, TX, USA

<sup>9</sup>Finnish Meteorological Institute, Helsinki, Finland

## Abstract:

The aim of this investigation is to carry out a study of the variability of nocturnal atmospheric turbulence at Jezero crater supported by modeling effort and monitored by MEDA. Although nighttime conditions in Mars' PBL are highly stable and turbulence is usually not expected, because of strong radiative cooling efficiently inhibiting convection, both observations and modeling shows the development of nighttime local turbulence. The rapid turbulent kinetic energy (hereafter TKE), wind and pressure fluctuations observed during nighttime both with MRAMS mesoscale modeling and MEDA is a clear indicative of nocturnal turbulence. The origin of this nocturnal turbulence is explored with MRAMS and, as opposed to Gale crater, low evidence of significant gravity waves activity during the whole period studied was found. On the contrary, the nighttime turbulence at Jezero crater could be shear driven and may be explained due to an enhanced mechanical turbulence produced by increasingly strong shear (onset of a strong low-level jet) at the nocturnal inversion interface. As the nocturnal inversion develops, the winds above become decoupled from the surface and the decrease in friction produces a net acceleration. Once the critical Richardson Number is reached ( $Ri \sim < 0.25$ ), shear instabilities can mix warmer air aloft down to the surface. A dustier atmosphere contributes to nighttime turbulence strengthening the nighttime low-level jet and weakening the near-surface atmospheric stability.

## 1. Introduction

The Mars 2020 Perseverance rover landed in Mars in February 2021 at 18.44°N 77.45°E within and near the northwest rim of Jezero crater. The MEDA sensor suite aboard Perseverance rover [1] includes a dust and optical radiation sensor (RDS) with a dedicated camera (SkyCam), a pressure sensor (PS), a relative humidity sensor (HS), a wind sensor (WS), five air temperature sensors (ATS), and a thermal infrared sensor for upwelling infrared flux and ground temperature determination (TIRS). MEDA acquires data typically over 50% of a full sol. After more than 380 sols in Mars, the data allows to explore the changing dynamics of the Martian atmosphere from northern Spring ( $Ls=5^\circ$ , sol 1) to northern Autumn Equinox ( $Ls=180^\circ$ , sol 361) and beyond.

## 2. MRAMS mesoscale simulations design

In an effort to better understand the different me-

teorological environments inside Jezero crater, MRAMS was applied to Mars 2020 landing site region using nested grids with a spacing of 330 meters on the innermost grid that is centered over the landing site [2]. MRAMS is ideally suited for this investigation; the model is explicitly designed to simulate Mars' atmospheric circulations at the mesoscale and smaller with realistic, high-resolution surface properties. The model is run for 4 sols with 4 grids and then the 3 additional grids are added and run for at least 3 more sols. Initialization and boundary condition data are taken from a NASA Ames GCM simulation with column dust opacity driven by zonally-averaged TES retrievals. Vertical dust distribution is given by a Conrath-v parameterization that varies with season and latitude. The lowest thermodynamic level (where temperature and pressure are prognosed) is  $\sim 14$ m above the ground. Ideally, the first vertical level would be located at the height of the MEDA sensors, but this is not computationally practical.

## 3. Nighttime turbulence modeled with MRAMS

The effect of subgrid-scale eddies is captured within MRAMS via a prognostic TKE (Figure 1) equation [3]. MRAMS shows a peak in TKE during the afternoon, which is consistent with the modeled high-frequency variations in air temperatures [2, Figure 4]. The sudden increase in air temperature during the evenings [2, Figure 4] at the onset of radiative cooling is produced by mechanically driven turbulence since the atmosphere is stable and non-convective in the evening (Figure 2).

The model does often show small increases of TKE during the night (Figure 1), especially during  $Ls=180^\circ$  (corresponding to Mars 2020 sol 362) and some during  $Ls$  105 and  $Ls$  160 (corresponding to Mars 2020 sols 216 and 326), that could be associated with the turbulent aspects of the nighttime dynamical flows when compared with nearby locations with more flat topography. During the late evening and night, MRAMS is resolving thermal variations

[2, Figure 4] and does often show small increases of TKE at that time (Figure 1). The rapid air temperature fluctuations modeled at night in all seasons is indicative of nocturnal turbulence.

There is low evidence of significant wave activity during the whole period studied and only some gravity waves were found. The nighttime turbulence could be attributed to shear driven turbulence and may be explained due to an enhanced mechanical turbulence driven by increasingly strong shear, with the onset of the nocturnal low-level jet, at the nocturnal inversion interface (an example on Figure 3). As the nocturnal inversion develops, the winds above become decoupled from the surface and the decrease in friction produces a net acceleration [4, 5, 6, 7]. Once the critical Richardson Number is reached ( $Ri \sim < 0.25$ , Figure 4), shear instabilities can mix warmer air aloft down to the surface [8, 9, 10].

The dustier atmosphere, when arrival of northern autumn equinox, also contributes to decrease the nighttime Richardson number by two means: strengthening of the nighttime low-level jet deepening the near-surface wind shear and weakening near-surface atmospheric stability by increasing the nighttime surface temperature and decreasing of atmospheric temperature.

A third possible strengthening of the nighttime turbulence at Jezero could be the convergence, after 01:00 LSTS, of downslope winds blowing from NW rim fighting against SE winds blowing both from east crater rims and from Jezero mons (located SE outside the crater), producing a big whirlpool inside the crater (Figure 5) that could be the responsible of the high variability of wind directions observed by MEDA.

### 3. Nighttime turbulence observed with MEDA

The rapid fluctuations of pressure (moreover during high dust periods), TKE (derived only with horizontal wind speeds, that will be updated with vertical winds in the future) and wind speeds observed during nighttime with MEDA (Figures 6, 7 and 8) is a clear indicative of nocturnal turbulence. There are two higher turbulence periods around sol #78 ( $\sim Ls=42^\circ$ ) and around sol #290 ( $\sim Ls=141^\circ$ ), and a lower turbulence period around sol #200 ( $\sim Ls=97^\circ$ , Figure 6 left) for the 20:00 to 00:00 period. After 01:00, the winds are very weak and all the correlations and mixings tend to be more diluted (Figure 6 right).

## 4. Figures

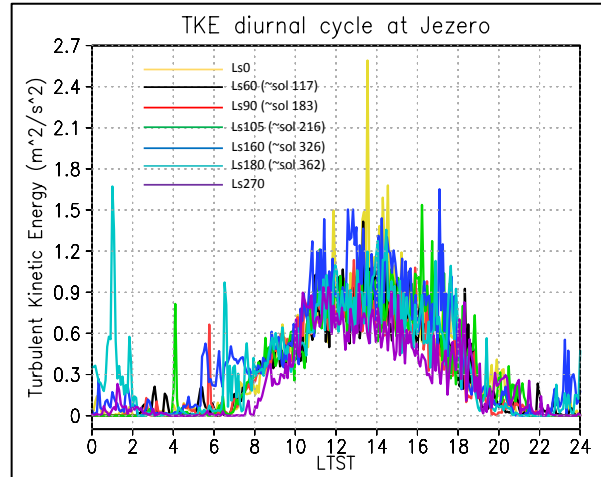


**Figure 1:** TKE diurnal cycle predicted with MRAMS for Jezero crater at Ls0, 60, 90, 105, 160, 180 and 270.

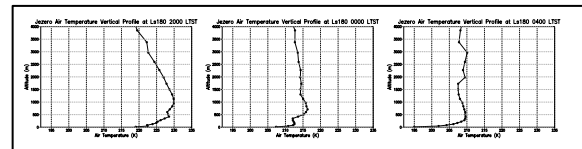


**Figure 2:** MRAMS vertical profiles of air temperature for Ls180 at Mars 2020 location corresponding to sol #362.

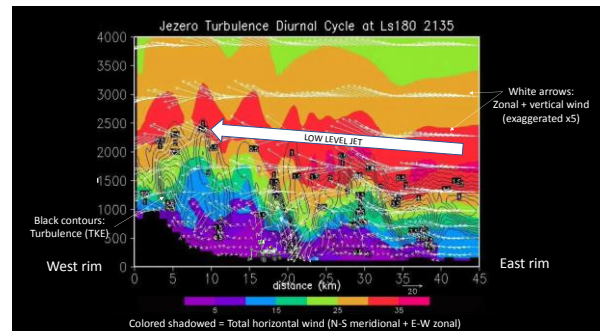


**Figure 3:** MRAMS vertical cross-section (Jezero's west rim to east rim) at 21:35 LTST of  $Ls=180^\circ$  - corresponding to Mars 2020 sol #362- of total wind (zonal + meridional) in colored shadowed, zonal + vertical (exaggerated x5) wind in white arrows and TKE in black contours. The west crater rim is the hill on the left. Perseverance rover is located at  $x \approx 17$  km. Shear instabilities mix warmer air aloft down to the surface.

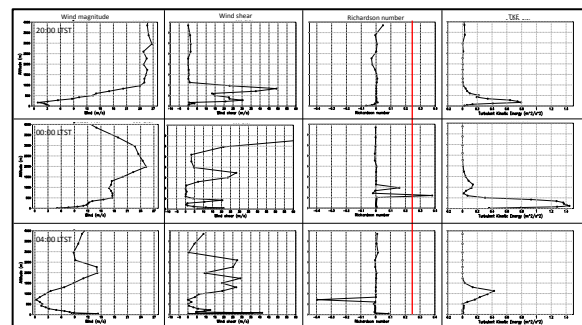


**Figure 4:** MRAMS vertical profiles of wind magnitude, wind shear, Richardson number (Ri) and TKE for Ls180 at Mars 2020 location corresponding to Mars 2020 sol #362 (Ls=180°). Once the critical Richardson Number is reached (Ri  $\sim$  < 0.25, red line), shear instabilities can mix warmer air aloft down to the surface.

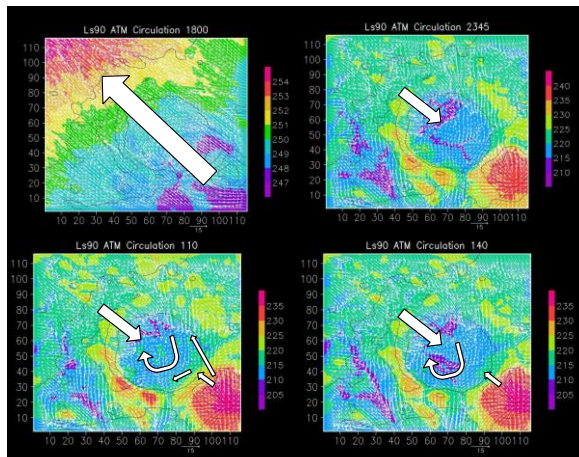


**Figure 5:** Near-surface winds (vectors) and potential temperature (shaded) as predicted on numerical grid 5. Vectors are plotted at every other grid point. Topography contours are shown in black. Wind vector scale is shown in the bottom right area of the panels. hh:mm LTST on the top right. A big whirlpool inside the crater could be the responsible of the high variability of wind directions observed by MEDA after 01:00 LTST.

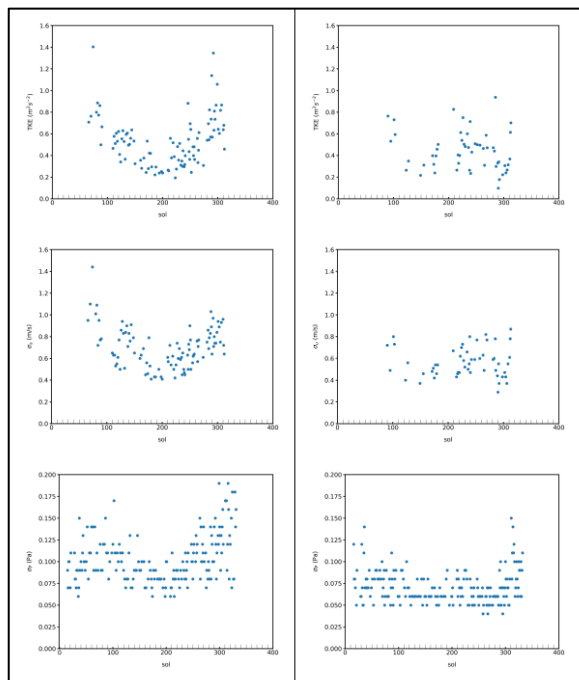


**Figure 6:** MEDA TKE (derived only with horizontal wind speeds, that will be updated with vertical winds in the future), wind speeds and pressure fluctuations averaged over 5 min for the periods 20:00 to 00:00

LTST (left) and 01:00 to 04:00 LTST (right). After 01:00, the winds are very weak and all the correlations and mixings tend to be more diluted.

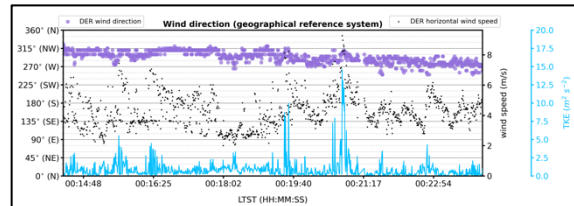


**Figure 7:** MEDA TKE (derived only with horizontal wind speeds, that will be updated with vertical winds in the future), wind direction and horizontal wind speed instantaneous (with a cadence of 1 Hz) measurements for the period 00:14 to 00:23 LTST at sol #73.

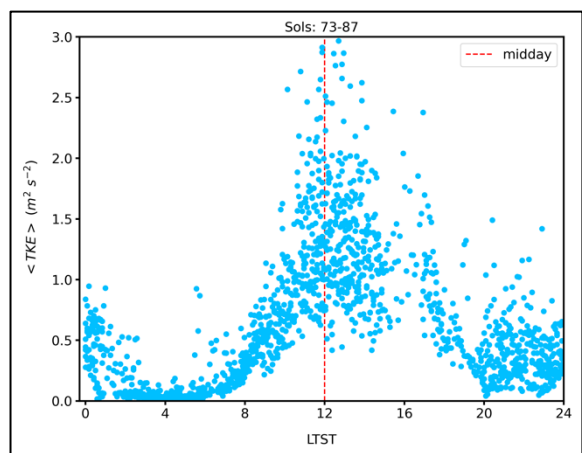


**Figure 8:** Diurnal cycle of MEDA TKE (derived only with horizontal wind speeds, that will be updated with vertical winds in the future) averaged over 5 min for sols #73-87.

## 5. References

[1] Rodriguez-Manfredi et al. 2020; [2] Pla-Garcia et al. 2021; [3] Mellor and Yamada 1974; [4] Davis 2000; [5] Blackadar 1957; [6] Thorpe and Guymer 1977; [7] Mahrt 1981; [8] Miles 1961; [9] Banfield et al. 2020; [10] Chatain et al. 2021